

First measurement of the antihelium-3 inelastic cross section and its implications for indirect dark matter searches

Laura Šerkšnytė^{a,*} for the ALICE collaboration

*^aThe Technical University of Munich ,
James-Franck-Str. 1, Garching, Germany*

E-mail: laura.serksnyte@tum.de

Cosmic ray antinuclei serve as a probe in the endeavour to indirectly detect dark matter particles, providing an almost background-free signal. Modelling cosmic-ray antinuclei fluxes requires input from nuclear physics experiments such as the production cross section and the inelastic cross section with matter. In this work, the first measurement of the inelastic antihelium-3 cross section utilizing the ALICE detector as a target material is presented. The resulting cross sections were employed to study the transparency of the Galaxy to the cosmic-ray antihelium-3 fluxes. The transparency for the cosmic ray flux stemming from dark matter annihilation was obtained to be around 50% in the entire energy range. In the case of the background component stemming from cosmic ray collisions with the interstellar medium, the transparency increases from 25% to 90% with increasing energy.

38th International Cosmic Ray Conference (ICRC2023)
26 July - 3 August, 2023
Nagoya, Japan



*Speaker

1. Introduction

The yet undetected dark matter constitutes around 27% [1] of our Universe. Some dark matter candidates, such as Weakly Interacting Massive Particles (WIMPs), are expected to annihilate to ordinary matter, including antinuclei such as antihelium-3. The antinuclei produced in our Galaxy would propagate in the Galactic magnetic fields. They could reach Earth and be measured as cosmic rays with dedicated detectors, such as AMS-02 [2] or GAPS [3]. The kinetic-energy distribution of such antihelium-3 cosmic rays is expected to peak at around 1 GeV/A. The only other known process to produce antinuclei in our Galaxy is cosmic-ray collisions with interstellar gas. However, such a background component is expected to have a kinetic energy distribution peaked at around 10 GeV/A, resulting in a high signal-to-background ratio at kinetic energies around 1 GeV/A. Modelling cosmic ray antihelium-3 fluxes requires solving the transport equation which accounts for their production, propagation and possible inelastic interactions with interstellar gas. The propagation parameters are the same for all cosmic-ray species and thus can be constrained by available cosmic-ray measurements such as proton flux and boron-to-carbon ratio [4]. However, the production and inelastic cross sections of antinuclei must be measured at accelerator experiments on Earth. The production of light (anti)nuclei has been and still is studied by many experiments, including ALICE [5–7], STAR [8, 9], NA44 [10], PHENIX [11] and others [12–15], while the antihelium-3 inelastic cross section with matter has never been measured.

The inelastic cross section is usually measured by impinging a particle beam of interest on a target. As no antihelium-3 beams are available, new techniques to measure the inelastic cross section were developed by studying antihelium-3 nuclei produced in the collisions at the Large Hadron Collider (LHC) and utilising the ALICE detector as a target material. One of the techniques is based on measuring the antimatter-to-matter ratio and has already been employed for antideuteron studies [16]. The other technique identifies antihelium-3 reconstructed in Time-Of-Flight (TOF) and Time-Projection-Chamber (TPC) detectors and evaluates how many antinuclei disappeared in the detector material between them. The resulting inelastic cross sections were then used to model cosmic-ray antihelium-3 fluxes and to evaluate the transparency of our Galaxy. For this purpose, antinuclei were implemented in publicly available GALPROP software¹ [17] within the scope of this work. In the following, the details and results of antihelium-3 inelastic cross section measurement and the modelling of the cosmic-ray antihelium-3 fluxes are discussed.

2. Determining the antihelium-3 inelastic cross sections with ALICE

LHC is known as an antimatter factory, producing the same amount of antimatter and matter at its high collision energies. The produced antinuclei can be measured by the ALICE detector which also serves as a target material. The inelastic antihelium-3 cross section can be determined in such a setup with two complementary methods.

The first method is based on antimatter-to-matter ratio measurement. The primordial ratio of antihelium-3 to helium-3 has been derived from precise antiproton-to-proton ratio measurements [18, 19] and corresponds to 0.994 ± 0.045 [20] in pp collisions at the centre-of-mass energy $\sqrt{s} = 13$ TeV.

¹Code and documentation available at <https://galprop.stanford.edu>.

However, the reconstructed ratio is different as antihelium-3 has a higher probability than helium-3 of interacting with the detector material (a possible scenario is shown in Fig. 1). The reconstructed ratio can be expressed as

$$\frac{{}^3\overline{\text{He}}}{{}^3\text{He}} = \left(\frac{{}^3\overline{\text{He}}}{{}^3\text{He}} \right)_{\text{prim}} \cdot \exp \left(-\alpha (\sigma_{\text{inel}}^{{}^3\overline{\text{He}}} - \sigma_{\text{inel}}^{{}^3\text{He}}) \Delta x \right). \quad (1)$$

Here, $\left(\frac{{}^3\overline{\text{He}}}{{}^3\text{He}} \right)_{\text{prim}}$ is the primordial ratio. The exponential considers the probability for nuclei and antinuclei to interact with detector material while traversing path length Δx and disappear. The detector material is described via $\alpha = \rho N_A / M$ term, where N_A is the Avogadro's number, ρ is the density and M is the molar mass of the target. The inelastic cross sections of helium-3 and antihelium-3 with matter are denoted as $\sigma_{\text{inel}}^{{}^3\overline{\text{He}}}$ and $\sigma_{\text{inel}}^{{}^3\text{He}}$, respectively. The helium-3 inelastic cross section is rather well known; thus, the measurement of the reconstructed antimatter-to-matter ratio allows us to determine the antihelium-3 inelastic cross section. However, performing such studies

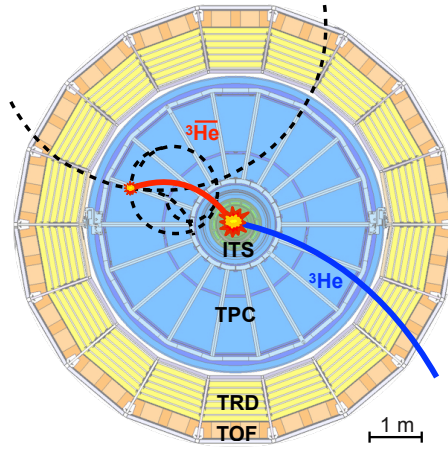


Figure 1: Schematic of the relevant for presented analyses ALICE detectors in the plane perpendicular to the beam axis [20]. The collision point is located at the centre and the ITS, TPC, TRD and TOF detectors are depicted in green, blue, yellow and orange colours, respectively. The blue and red lines show possible helium-3 and antihelium-3 paths. Here, the helium-3 traverses detector without inelastic interactions, while the antihelium-3 annihilates in the TPC gas and produces charged particles shown as dashed lines.

requires good detector geometry and material budget knowledge. The ALICE detector and its performance have been described in Refs. [21, 22], while the material budget has been studied in Ref. [23]. The inelastic cross section can be obtained by comparing the measured antimatter-to-matter ratio values in each momentum bin to full-pledged ALICE detector simulations, where the inelastic cross sections can be freely varied. For this purpose, the GEANT4 package [24, 25] was utilised. The momentum p is measured via the determination of the track curvature in the ALICE magnetic field ($B = 0.5$ T), while the particle identification is performed via the measurement of their specific energy loss (dE/dx) in the TPC detector gas. If only the TPC information is required for the track reconstruction, the inelastic cross section measurement is sensitive only to the material budget of ITS and TPC detectors. However, the higher momentum antinuclei are also required

to have a hit in the TOF detector, ensuring that the detected antihelium-3 traversed not only ITS and TPC detectors but also the Transition-Radiation-Detector (TRD). This results in two effective average targets: ITS+TPC with averaged atomic mass $\langle A \rangle = 17.4$ and ITS+TPC+TRD with $\langle A \rangle = 31.8$. The details of the particle reconstruction, systematic uncertainties and measured antimatter-to-matter ratio can be found in Ref. [20]. The determined antihelium-3 inelastic cross section is shown in the left panel of Fig. 2, where the full circles correspond to the central value and yellow boxes to the total 1σ uncertainty. The arrow shows the 95% confidence limit. The dashed line depicts the GEANT4 inelastic cross section based on the Glauber model for average target material with $\langle A \rangle = 17.4$ and solid line shows the case of $\langle A \rangle = 31.8$. The GEANT4 prediction agrees with the data.

The second method to determine antihelium-3 inelastic cross section requires measuring the number of antihelium-3 reconstructed in the TOF and TPC detectors. As shown in Fig. 1, the TRD is located between the TPC and TOF detectors acting as a target material for the traversing antihelium-3. The ratio of antihelium-3 reconstructed in TOF and TPC detectors thus allows to determine its inelastic cross section with matter. For this purpose, the measured ratio is compared to the GEANT4 simulations, where the inelastic cross section can be varied. This method was applied to analyse the Pb-Pb collisions at $\sqrt{s_{NN}} = 5.02$ TeV. The details of reconstruction, systematic uncertainties and the measured ratios can be found in Ref. [20]. The determined antihelium-3 inelastic cross sections are shown in the right panel of Fig. 2. The full circles correspond to the central value while the pink boxes show 1σ uncertainty. The dashed line depicts GEANT4 inelastic cross section for the averaged target material corresponding to TRD detector with $\langle A \rangle = 34.7$. The GEANT4 prediction is in good agreement with the experimentally determined values.

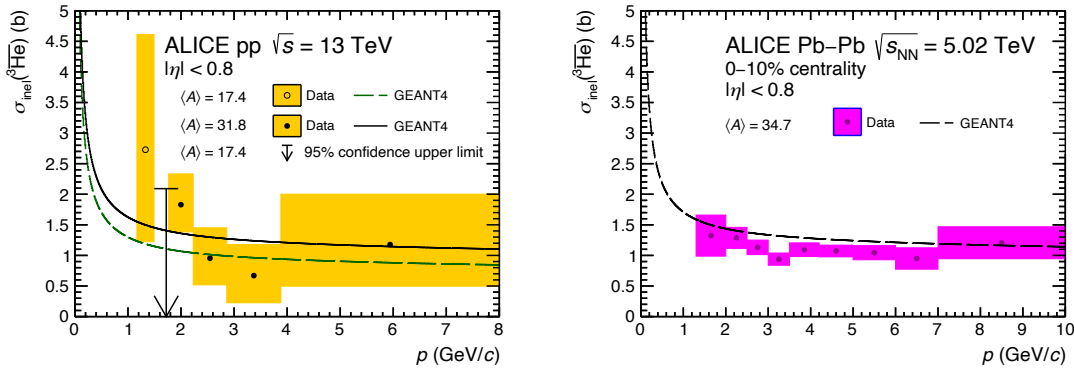


Figure 2: Resulting antihelium-3 inelastic cross-section obtained with antimatter-to-matter (left) and TOF-to-TPC (right) methods [20]. The yellow and pink boxes correspond to 1σ uncertainty and the black circles to the central value. The dashed and solid lines represent GEANT4 cross sections on the averaged target material. The different $\langle A \rangle = 17.4$ values correspond to the different effective targets.

In the Galaxy, the most contributing targets are the hydrogen and helium gas. Thus our measurement has to be extrapolated to the lighter targets. For this purpose, the GEANT4 package was employed and its default values were corrected with a scaling factor based on our data (ratio of measured cross sections and GEANT4). The default GEANT4 inelastic cross sections for antihelium-3 on proton targets is shown in Fig. 3 as red line, while the one corrected by our measurement is

depicted as the green band which includes the 1σ experimental uncertainty and additional 8% uncertainty induced by the usage of GEANT4 to extrapolate to the light targets. Same procedure is performed for helium-4 targets.

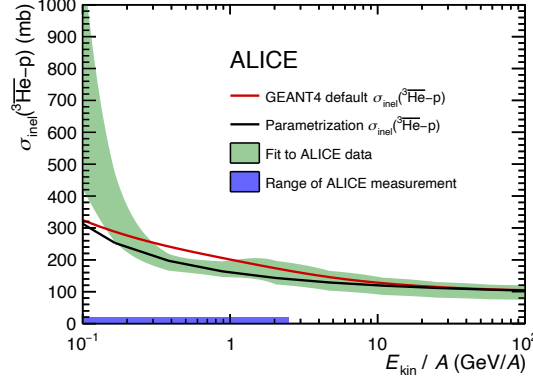


Figure 3: The antihelium-3 inelastic cross section taken from GEANT4 (red line), corrected based on our measurement (green band) and as estimated in previous cosmic ray studies (black band) [20].

3. Determining the cosmic ray antihelium-3 fluxes and the transparency of the Galaxy

The cosmic ray fluxes were obtained with GALPROP package which solves the transport equation. The latter provides the time dependent cosmic ray density per unit of the total particle momentum $\psi = \psi(\mathbf{r}, p, t)$ as

$$\frac{\partial \psi}{\partial t} = q(\mathbf{r}, p) + \mathbf{div}(D_{xx} \mathbf{grad} \psi - \mathbf{V} \psi) + \frac{\partial}{\partial p} p^2 D_{pp} \frac{\partial \psi}{\partial p} - \frac{\partial}{\partial p} \left[\psi \frac{dp}{dt} - \frac{p}{3} (\mathbf{div} \cdot \mathbf{V}) \psi \right] - \frac{\psi}{\tau}. \quad (2)$$

Here, $q(\mathbf{r}, p)$ is the antihelium-3 source function. Such source functions were implemented for the cosmic ray collisions with interstellar medium and dark matter annihilations in GALPROP, as these are not part of the official package. The source function for cosmic ray collisions with interstellar medium depends on the interstellar gas and cosmic ray distributions, and the antihelium-3 production cross section. The gas and cosmic ray distributions are already part of GALPROP while the production cross sections were implemented based on Ref. [26] and include p-p, p-He, He-p and He-He collisions. The source for dark matter annihilation was implemented assuming Navarro-Frenk-White dark matter density profile [27] for 100 GeV mass dark matter particles annihilating through W^+W^- channel, employing dark matter thermally averaged annihilation cross section value of $\langle \sigma v \rangle = 2.6 \times 10^{-26} \text{ cm}^3 \text{ s}^{-1}$ [2] and the antihelium-3 production cross sections based on Ref. [28]. The propagation parameters D_{xx} , \mathbf{V} and D_{pp} correspond to the spatial diffusion coefficient, the convection velocity and the diffusive re-acceleration coefficient, respectively. These parameters are the same for all cosmic-ray species and thus can be constrained to available cosmic ray measurements. In our work, parameters obtained in Ref. [4] were employed. The $-\frac{\psi}{\tau}$ term accounts for the particle loss via inelastic collisions with interstellar gas as

$$\frac{1}{\tau} = \beta c \left(n_H(\mathbf{r}) \sigma_{\text{inel}}^{3\overline{\text{He}}p}(p) + n_{He}(\mathbf{r}) \sigma_{\text{inel}}^{3\overline{\text{He}}^4\text{He}}(p) \right), \quad (3)$$

where $n_H(\mathbf{r})$ and $n_{He}(\mathbf{r})$ are the densities of hydrogen and helium-4 gas in the Galaxy. The antihelium-3 inelastic cross sections on such gas targets $\sigma_{\text{inel}}^{3\text{He}p}(p)$ and $\sigma_{\text{inel}}^{3\text{He}^4\text{He}}(p)$ can be constrained by our measurement. The resulting local interstellar cosmic ray fluxes are shown in the left upper panel of Fig. 4. To compare the obtained fluxes to the sensitivities of GAPS and AMS-02 detectors, the local interstellar fluxes have to be corrected for the solar modulation effects which was done employing the Force-Field approximation with the modulation potential of 400 MeV [29]. The resulting solar modulated fluxes are shown in the right upper panel of Fig. 4. The dashed lines depict fluxes obtained assuming no inelastic interaction of antihelium-3 with interstellar gas. The solid lines correspond to fluxes obtained employing the default GEANT4 inelastic cross sections, while the band shows results when GEANT4 values are corrected based on our measurements as described above.

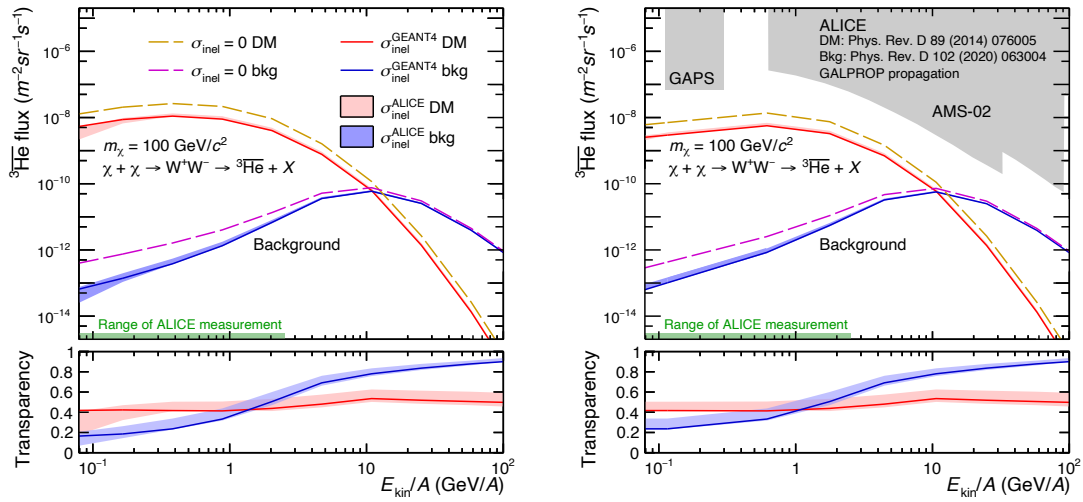


Figure 4: Upper panels: Cosmic ray fluxes stemming from dark matter annihilation (depicted in red and orange colours) and cosmic ray collisions with interstellar medium (depicted in blue and violet colours) [20]. The dashed lines correspond to the assumption of no antihelium-3 inelastic interactions in the interstellar medium, while the solid lines show results obtained modelling inelastic interactions based on GEANT4 cross sections. The corresponding bands were obtained by correcting the GEANT4 values based on our measurement. For details refer to the text.

The antihelium-3 fluxes depicted in red and orange colours are stemming from dark matter annihilation while the fluxes shown in violet and blue colours correspond to the antihelium-3 flux from cosmic ray collisions with interstellar medium. A high signal-to-background ratio is obtained for kinetic energies below few GeV/A. The lower panels show the obtained transparency. Transparency is defined as the ratio of the flux obtained with specific inelastic cross section and the flux assuming no inelastic interactions. It shows the fraction of particles which manage to reach the Earth environment without annihilating in the interstellar medium. After solar modulation, the transparency for dark-matter component of around 50% (blue band) is obtained if inelastic interactions are evaluated based on our inelastic cross section measurements. Similar result is obtained with default GEANT4 values (blue line). For the background component, the transparency increases from around 25% to 90% with increasing kinetic energy (red band and line). Our results

show that the Galaxy is transparent to the cosmic ray antihelium-3 propagation and provide the first ever estimate of the uncertainty on the fluxes stemming from inelastic cross section measurement.

4. Summary

The first ever measurement of the antihelium-3 inelastic cross section was performed employing the ALICE detector as a target material based on two methods. The obtained inelastic cross sections were then used to study cosmic ray antihelium-3 fluxes and the transparency of the Galaxy to the propagation of such antinuclei. The transparency of 50% was obtained for the dark matter annihilation component and the increasing transparency from 25% to 90% with increasing kinetic energy was estimated for the background component. Our result shows that, indeed, the Galaxy is transparent to the cosmic ray antihelium-3 and thus such antinuclei could be measured at Earth.

References

- [1] Planck Collaboration, *Planck 2018 results. VI. Cosmological parameters*, *Astron. Astrophys.* 641, A6 (2020).
- [2] Korsmeier, M., Donato, F. Fornengo, N., *Prospects to verify a possible dark matter hint in cosmic antiprotons with antideuterons and antihelium*, *Phys. Rev. D* 97, 103011 (2018).
- [3] GAPS Collaboration, *Cosmic antihelium-3 nuclei sensitivity of the GAPS experiment*, *Astropart. Phys.* 130, 102580 (2021).
- [4] Boschini, M. et al., *Inference of the local interstellar spectra of cosmic-ray nuclei $Z \leq 28$ with the GalProp–HelMod framework*, *Astrophys. J. Suppl.* 250, 27 (2020).
- [5] ALICE Collaboration, *Production of light nuclei and anti-nuclei in pp and Pb-Pb collisions at energies available at the CERN Large Hadron Collider*, *Phys. Rev. C* 93, 024917 (2016).
- [6] ALICE Collaboration, *Measurement of deuteron spectra and elliptic flow in Pb–Pb collisions at $\sqrt{s_{NN}} = 2.76$ TeV at the LHC*, *Eur. Phys. J. C* 77, 658 (2017).
- [7] ALICE Collaboration, *Multiplicity dependence of (anti-)deuteron production in pp collisions at $\sqrt{s} = 7$ TeV*, *Phys. Lett. B* 794, 50–63 (2019).
- [8] STAR Collaboration, *Observation of the antimatter helium-4 nucleus*, *Nature* 473, 353–356 (2011).
- [9] STAR Collaboration, *\bar{d} and ${}^3\bar{He}$ production in $\sqrt{s_{NN}} = 130$ GeV Au+Au collisions*, *Phys. Rev. Lett.* 87, 262301 (2001); erratum 87, 279902 (2001).
- [10] NA44 Collaboration, *Deuteron and anti-deuteron production in CERN experiment NA44*, *Nucl. Phys. A* 590, 483C–486C (1995).
- [11] PHENIX Collaboration, *Deuteron and antideuteron production in Au + Au collisions at $\sqrt{s_{NN}} = 200$ GeV*, *Phys. Rev. Lett.* 94, 122302 (2005).

- [12] E864 Collaboration, *Anti-deuteron yield at the AGS and coalescence implications*, Phys. Rev. Lett. 85, 2685–2688 (2000).
- [13] NA49 Collaboration, *Energy and centrality dependence of deuteron and proton production in Pb + Pb collisions at relativistic energies*, Phys. Rev. C 69, 024902 (2004).
- [14] CLEO Collaboration, *Anti-deuteron production in $\Upsilon(nS)$ decays and the nearby continuum*, Phys. Rev. D 75, 012009 (2007).
- [15] ALEPH Collaboration, *Deuteron and anti-deuteron production in e^+e^- collisions at the Z resonance*, Phys. Lett. B 639, 192–201 (2006).
- [16] ALICE Collaboration, *Measurement of the low-energy antideuteron inelastic cross section*, Phys. Rev. Lett. 125, 162001 (2020).
- [17] Strong, A. and Moskalenko, I., *Propagation of cosmic-ray nucleons in the Galaxy*, Astrophys. J. 509, 212–228 (1998).
- [18] ALICE Collaboration, *Mid-rapidity anti-baryon to baryon ratios in pp collisions at $\sqrt{s} = 0.9, 2.76$ and 7 TeV measured by ALICE*, Eur. Phys. J. C 73, 2496 (2013).
- [19] ALICE Collaboration, *Midrapidity antiproton-to-proton ratio in pp collisions at $\sqrt{s} = 0.9$ and 7 TeV measured by the ALICE experiment*, Phys. Rev. Lett. 105, 072002 (2010).
- [20] ALICE Collaboration, *Measurement of anti- ^3He nuclei absorption in matter and impact on their propagation in the Galaxy*, Nature Physics 19, 61–71 (2023)
- [21] ALICE Collaboration, *The ALICE experiment at the CERN LHC*, JINST 3, S08002 (2008).
- [22] ALICE Collaboration, *Performance of the ALICE experiment at the CERN LHC*, Int. J. Mod. Phys. A29, 1430044 (2014).
- [23] ALICE Collaboration, *Validation of the ALICE material budget between TPC and TOF detectors*, ALICE-PUBLIC-2022-001 (CERN, 2022).
- [24] Geant4 Collaboration, *Geant4—a simulation toolkit*, Nucl. Instrum. Meth. Phys. Res. A A506, 250–303 (2003).
- [25] Uzhinsky, V., *Antinucleus–nucleus cross sections implemented in Geant4*, Phys. Lett. B705, 235–239 (2011).
- [26] Shukla, A. et al., *Large-scale simulations of antihelium production in cosmic-ray interactions*, Phys. Rev. D 102, 063004 (2020).
- [27] Navarro, J. F., Frenk, C. S. and White, S. D., *The structure of cold dark matter halos*, Astrophys. J. 462, 563–575 (1996).
- [28] Carlson, E. et al., *Antihelium from dark matter*, Phys. Rev. D 89, 076005 (2014).
- [29] Gleeson, L. and Axford, W., *Solar modulation of Galactic cosmic rays*, Astrophys. J. 154, 1011–1026 (1968).